Ordering and finite-size effects in the dynamics of one-dimensional transient patterns

A. Amengual, E. Hernández-García, and M. San Miguel
Departament de Física, Universitat de les Illes Balears, E-07071 Palma de Mallorca, Spain
(Received 9 October 1992)

We introduce and analyze a general one-dimensional model for the description of transient patterns which occur in the evolution between two spatially homogeneous states. This phenomenon occurs, for example, during the Fréedericksz transition in nematic liquid crystals. The dynamics leads to the emergence of finite domains that are locally periodic and independent of each other. This picture is substantiated by a finite-size scaling law for the structure factor. The mechanism of evolution towards the final homogeneous state is by local roll destruction and associated reduction of local wave number. The scaling law breaks down for systems of size comparable to the size of the locally periodic domains. For systems of this size or smaller, an apparent nonlinear selection of a global wavelength holds, giving rise to long-lived periodic configurations which do not occur for large systems. We also make explicit the unsuitability of a description of transient pattern dynamics in terms of a few Fourier mode amplitudes, even for small systems with a few linearly unstable modes.

PACS number(s): 47.20.Hw, 47.20.Ky, 61.30.Gd

I. INTRODUCTION

The most simple situation considered in the context of pattern-formation studies [1] is the one in which a homogeneous stable steady state of a system becomes unstable at a threshold value of a control parameter, so that beyond threshold the new stable state is time independent and with a well-defined spatial periodicity. In such a situation it is first generally aimed to describe some static properties, such as the threshold value of the control parameter, possible wavelengths of the pattern, and possible higher-order bifurcations. Another set of interesting questions is associated with the transient dynamics of the pattern-formation process given an initial unstable homogeneous state [2]. A different physical situation is the one of transient pattern formation during the temporal evolution between two homogeneous steady states: In this case an homogeneous stable steady state becomes unstable beyond a given threshold and the transient evolution to the final homogeneous stable steady state involves a process of pattern growth and decay. Most of the usual mathematical techniques used to describe the first situation seem to fail for problems involving transient pattern dynamics.

Transient pattern formation is well documented from the experimental point of view for different instabilities in nematic liquid crystals [3, 4]. A typical situation is the magnetic Fréedericksz transition in which for a large enough applied magnetic field, the nematic director does not reorientate homogeneously, but a striped pattern with a characteristic wavelength emerges. This pattern can last from minutes to hours depending on the specific geometry and the material, but it finally disappears leading to the homogeneously reoriented final equilibrium state. For most geometries of the system, the pattern admits a good description by one-dimensional models. A good summary of different situations considered in this context is given in Ref. [4]. Generally speaking, the transient pattern is associated with the coupling of the director field with hydrodynamic variables so that the fastest response to the applied field is not homogeneous in space [5]. A mechanism of wavelength selection based on this idea of fastest response has been proposed [3–7]: the well-defined observed periodicity has been associated with the mode of fastest growth and its dependence with the applied magnetic field has been considered theoretically and experimentally. However, a nonlinear mechanism of wavelength selection has also been invoked and substantiated by some experimental and restricted numerical studies [8]. The process of pattern formation in nematic liquid crystals can be described in detail through the full set of nematic hydrodynamic equations [9], which have been consistently formulated also in the presence of thermal fluctuations [6]. Such equations have been discussed in a variety of situations [3, 4, 7, 8]. These detailed discussions of a rather complicated set of equations might hide some general features of the problem of transient pattern formation and development. Our aim in this paper is to propose and analyze a generic model for one-dimensional transient pattern formation which describes general features of these problems. It is obvious that a precise comparison with experiment would require the consideration of some specific details. Nevertheless, we hope that general aspects as wavelength selection (if such selection does occur), mechanisms of pattern evolution, and the important issue of finite-size effects can be understood from this general model.

The model we analyze is defined by the following equation for a scalar variable $\theta(x,t)$:

$$\dot{\theta}(x,t) = (a - \partial_x^2)(\partial_x^2\theta + c\theta - b\theta^3) \quad . \tag{1}$$

The dot denotes temporal derivative. The linearized ver-

sion of this equation in Fourier space

$$\dot{\theta}_q = \omega(q)\theta_q \tag{2}$$

involves an amplifying factor

$$\omega(q) = (a+q^2)(c-q^2) \ . \tag{3}$$

As seen in Fig. 1, this factor is such that for $c > 0$ there is a range of unstable modes for which $\omega(q) > 0$. If $a < 0$ the range of unstable modes does not include the mode $q = 0$ and the linear regime is qualitatively the same as for the well-known Swift-Hohenberg equation [10] used to describe the formation of stationary patterns. Here we are interested in the situation in which $a > 0$ for which the range of unstable modes is $(-q_c, q_c)$, with $q_c \equiv c^{1/2}$. If, in addition, $a < c$, the mode of fastest growth becomes different from zero: $q_m = [(c-a)/2]^{1/2}$. This implies the existence of an instability that for $0 < a < c$ involves the linear growth of a pattern with a characteristic periodicity given by q_m. Throughout the paper we fix $c \equiv 1$ and study (1) with periodic boundary conditions.

Equation (1) can be motivated as an approximation to the complete nematodynamic equations describing the magnetic Fréedericksz transition in a nematic. Under ordinary assumptions for the twist geometry [9] one obtains coupled equations for the angle orientation $\theta(x)$ of the director and a component of the velocity field, both in a plane in the middle of the sample. The approximation of negligible inertia permits the elimination of the velocity variable. This gives rise to an effective wave-number-dependent viscosity which appears as a q-dependent kinetic coefficient [6]. For small deformations θ and in the small wave-number limit [11, 12] one recovers Eq. (1), where the factor $(a - \partial_x^2)$ is the remaining part of the effective viscosity [13].

Within the context of model (1), we address in this paper three general questions associated with transient patterns dynamics in the intermediate nonlinear regime after the initial pattern emergence and before the late stages in which it disappears. The first question is the domain of validity of the linear theory and the possible existence of a wavelength-selection principle in the nonlinear regime. The second question is the characterization of the mechanism governing pattern evolution. Third we examine finite-size effects which could be preponderant

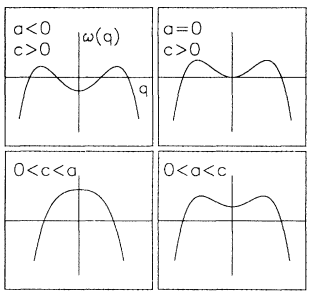

FIG. 1. The amplifying factor $\omega(q)$ of Eq. (3) in four different cases. See text for details.

in the question of a nonlinear selection principle. Our results indicate that for large systems a wavelength is initially selected in the linear regime but, on the average, it then changes monotonically in time approaching a final homogeneous state. During this evolution the system can be described as composed of several regions which evolve independently of each other. A local mechanism of roll destruction operates in such regime. This description is substantiated by giving evidence of a factorization of the size dependence of the structure factor for systems of different size. This factorization reveals the presence of uncorrelated regions of a characteristic length. This length is essentially time independent in the regime of dynamical evolution examined. For systems of size comparable or smaller than this length an apparent nonlinear selection of a wavelength occurs: configurations of well defined periodicity, which is not the one linearly selected, last for very long times, before evolving to the final homogeneous state. The reason why such periodic configurations are long lived is that they correspond to unstable stationary solutions which, for small system sizes, are approached in the initial transient regime. For large system sizes such configurations are not approached in the dynamical evolution from a typical initial configuration. A characteristic of small systems is that a very small number of modes are linearly unstable at $t = 0$ so that a description in terms of coupled ordinary differential equations for the amplitude of a few modes seems natural. We show that such description can give qualitatively wrong results. The basic simple reason for this fact is that such modes are not stabilized by nonlinear terms in the full equation, because they are not associated with stable solutions.

We finally wish to mention the relation of our analysis with another well-known physical situation in which transient patterns occur, namely spinodal decomposition [14]. The process of phase separation of a binary mixture quenched to a temperature below the critical temperature also displays a transient pattern with a time-dependent characteristic length. This analogy was pointed out many times [3]. However, in addition to differences in time scales [6], there is another important difference between this problem and the one of transient patterns in nematic liquid crystals and it is that the dynamics of spinodal decomposition is constrained by a conservation law. The initial [6, 15] and very late stages [11] of pattern dynamics in the magnetic Fréedericksz transition have been already studied in some detail by analogy with the problem of spinodal decomposition, but no detailed study seems available for the $d = 1$ intermediate nonlinear regime in which we are here interested

The outline of this paper is as follows. In Sec. II, we discuss the main characteristics of the model given by (1) and its stationary configurations, then we compare it with other related models. Section III describes our numerical results for large systems. Finally the description of a small system in terms of the amplitudes of a few modes is discussed in Sec. IV. Throughout the paper we restrict ourselves to $d = 1$ and we neglect thermal fluctuations. The role of fluctuations and two dimensional effects will be analyzed elsewhere.

II. A MODEL FOR GENERIC ASPECTS OF TRANSIENT PATTERN FORMATION

A first important property of the model given by Eq. (1) is that it can be written in a potential form

$$\dot{\theta}(x) = -\Gamma \frac{\delta F[\theta]}{\delta \theta(x)} \ , \tag{4}$$

where the kinetic coefficient Γ is the operator

$$\Gamma = a - \partial_x^2 \ , \tag{5}$$

and $F[\theta]$ is

$$F[\theta] = \int dx \ \left[-\frac{1}{2}\theta(x)^2 + \frac{b}{4}\theta(x)^4 + \frac{1}{2}|\partial_x \theta(x)|^2 \right] \ . \tag{6}$$

From (1) we can show that F is a good Lyapunov functional, in the sense that $dF/dt \leq 0$:

$$\frac{dF[\theta]}{dt} = \int dx \frac{\delta F[\theta]}{\delta \theta(x)} \dot{\theta}(x) = -\int dx \frac{\delta F[\theta]}{\delta \theta(x)} \Gamma \frac{\delta F[\theta]}{\delta \theta(x)} \leq 0 \ . \tag{7}$$

The last inequality holds because Γ is a positive definite operator (if $a > 0$), as can be seen from its expression in Fourier space.

The picture of the evolution is then that the system evolves, continuously decreasing $F[\theta]$, until a minimum of $F[\theta]$ is found, thus stopping the evolution. Note that such minima, stationary solutions of (1), are independent of Γ and of the parameter a and they are solutions of the simpler equation

$$\partial_x{}^2 \theta(x) + \theta(x) - b\theta(x)^3 = 0 \ . \tag{8}$$

An independent demonstration of the fact that with periodic boundary conditions the only stationary solutions of (1) (for $a > 0$) are those of (8) can be set up by writing (1) with $\dot{\theta}(x) = 0$ as the set of two equations:

$$\partial_x{}^2 \theta(x) + \theta(x) - b\theta(x)^3 = y(x) \ , \tag{9}$$

$$\Gamma y(x) = 0 \ . \tag{10}$$

Equation (10) is a linear second-order ordinary differential equation whose general solution is a linear combination of two exponentials. Only the combination leading to $y(x) = 0$ satisfies periodic boundary conditions, so that (9) reduces to (8). The qualitative features of all the stationary solutions of (1) can be discussed by writing (8) as [16]

$$\frac{d^2\theta(x)}{dx^2} = -\frac{dV(\theta)}{d\theta}, \tag{11}$$

which resembles a Newton equation for the motion of a particle of unit mass in a potential

$$V(\theta) = \frac{1}{2}\theta^2 - \frac{b}{4}\theta^4 \ , \tag{12}$$

the role of "time" being played by the coordinate x. From this analogy, the bounded solutions of (8) can be classified in three types: (a) the uniform solutions $\theta(x) = 1/\sqrt{b}$ and $\theta(x) = -1/\sqrt{b}$, (b) the uniform solution $\theta(x) = 0$, and (c) a family of solutions represented by nonlinear oscillations in the potential $V(\theta)$. The maximum possible frequency corresponds to oscillations of small amplitude, around $\theta = 0$, 2π being its period. The minimum frequency corresponds to trajectories in which $\theta(x)$ remains mostly near $\pm 1/\sqrt{b}$, with short excursions (domain walls) linking both states. In summary: there are periodic solutions to (8), which we denote by $\psi_q(x)$, each one containing a different fundamental wave number q and its harmonics, with $0 < q < 1$.

An important question is the linear stability of such stationary solutions. In order to consider this question, Eq. (8) does not contain enough information and the full dynamical equation (1), linearized around the stationary solution being checked, is needed. Linearization around the uniform solutions is immediate and it is found that the solution $\theta = 0$ is linearly unstable, and both $\theta = 1/\sqrt{b}$ and $\theta = -1/\sqrt{b}$ are linearly stable. These are also the absolute minima of the functional $F[\theta]$, so that they represent the stable equilibrium phases. The analysis of the stationary periodic solution $\psi_q(x)$, of fundamental wave number q, is performed with the introduction of $\theta(x,t) \equiv \psi_q(x) + \Delta(x,t)$ and linearization in Δ. The resulting equation is

$$\dot{\Delta}(x,t) = \Gamma \left[1 - 3b\psi_q(x)^2 + \partial_x{}^2 \right] \Delta(x,t) \ . \tag{13}$$

The general analysis of this linear equation with periodic coefficients requires of Bloch or Floquet theory [17]. A simplified situation was considered in [11] for the case in which q is small, so that the solution consisted basically of domains of the stable phases separated by thin domain walls. In that case it was found that the periodic solutions were linearly unstable. It can be generally shown that all the periodic solutions are unstable by studying its stability with respect to a uniform perturbation. The argument is as follows: Let us introduce the initial perturbation $\Delta(x, t = 0) = \Delta_0$, $\forall x$, and consider the initial time $t = 0^+$, when $\Delta(x,t) \approx \Delta_0$. Let be $x \equiv 0$ one of the places in which $\psi_q = 0$. Near $x = 0$, $\psi_q(x)^2$ will have a positive parabolic shape, so that $\partial_x^2[\psi_q(x \approx 0)^2] > 0$. Introducing this in Eq. (13) we find that $\mathrm{sgn}[\dot{\Delta}(x \approx 0, t = 0^+)] = \mathrm{sgn}[\Delta_0]$, showing the instability of ψ_q because a uniform initial perturbation grows. The consequence of the instability of *all* the periodic solutions is that none of them can represent the final state of the evolution, as long as a nonzero amplitude is given in the initial condition to the mode with wave number $q = 0$, or if noise is present in the system.

After this summary of the general properties of Eq. (1) it is interesting to compare them with the properties of other related models studied in the literature. To this end we write (1) (with $c = 1$) as

$$\dot{\theta} = -\partial_x^4 \theta + (a-1)\partial_x^2 \theta + a\theta - ab\theta^3 + b\partial_x^2 \theta^3 \ . \tag{14}$$

For $0 < a < 1$, the uniform solution $\theta = 0$ is unstable and the linear analysis predicts the growth of modes with wave number $q \neq 0$. It is then natural to relate this equa-

tion with others for which a periodic pattern grows from the unstable uniform solution. An archetypal example of such equations is the Swift-Hohenberg equation [10]

$$\dot{\theta} = [\gamma^2 - (1 + \partial_x^2)^2]\,\theta - b\theta^3 \quad . \tag{15}$$

The linear stability analysis of this equation leads in fact to the same linear growth spectrum as in Eq. (1), except for an important difference in sign in the regions around $q \sim 0$: the modes in this region slowly grow in our model ($a > 0$), whereas they are damped in the Swift-Hohenberg case (due to the fact that $0 < \gamma^2 < 1$). Other aspects of the initial stages in pattern development are qualitatively similar for both models. Another more fundamental difference is that the Swift-Hohenberg equation admits a family of *stable* periodic solutions, one of which will give the final state of the evolution, whereas (1) admits no stable solutions other than the uniform $\theta = \pm 1/\sqrt{b}$. This difference comes from a combination of the different sign of $\gamma^2 - 1$ versus a and of the additional term $\partial_x^2\theta(x)^3$ in (14). Thus, the evolution at late times will be completely different in both cases.

These differences have important methodological consequences: in order to study pattern formation in cases exemplified by the Swift-Hohenberg equation, a common strategy is to take as a small parameter the range of unstable modes around the most unstable one, which is small near a bifurcation point, and then obtain a nonlinear equation for the amplitude of the most unstable mode. The form of this equation is greatly determined by the symmetries of the problem, and by the assumption of being the first step in a uniform expansion. This strategy cannot be applied to our problem, because the characteristic shape of the linear instability spectrum in (3) with a fastest growing mode $q_m \neq 0$ is only obtained for $c > a$ which in our case (c=1) is far enough from the bifurcation point ($c = 0$), and the band of unstable wave numbers is as large as the wave number of the most unstable mode (because the mode with $q = 0$ has to be included in the description). Then bifurcation theory and normal forms are of no much help in our problem. In addition, the fact that the mode of fastest growth is not associated with a stable solution precludes the use of approximations based in the saturation of the linearly fastest growing mode, such as those in [18].

Another class of models with which it is natural to compare our model is the one represented by the Fisher-Kolmogorov equation, also known as Ginzburg-Landau equation for a real variable, or, with an added noise term, model A of critical dynamics [14, 19]:

$$\dot{\theta}(x,t) = \partial_x^2\theta(x) + \theta(x) - b\theta(x)^3 \quad . \tag{16}$$

The stationary solutions of this equation are exactly the same as in our model, and the only stable solutions are, as in our case, the uniform $\theta = \pm 1/\sqrt{b}$. In fact, the analysis in [11] shows that at very long times, the dynamics of the domain walls in (1) is the same as in (16). The main difference is, however, in the conditions created by the initial linear instability if $a < 1$: The fastest growing mode in (16) is always the one with wave number $q = 0$, which corresponds also to the final state. Then theories such as those in [18] are good descriptions of the evolution for all times.

In some sense, the time evolution of our model is a crossover between a linear behavior close to that in the Swift-Hohenberg model, and final stages similar to those in (16). Perhaps this is why the closest related model is the one represented by the Cahn-Hilliard equation, describing spinodal decomposition in binary mixtures and alloys. It is also known, when a noise term is added, as model B of critical dynamics [14, 19]. Formally, this model is obtained by putting $a = 0$ in Eq. (1). One-dimensional ($d = 1$) spinodal decomposition is physically artificial and consequently has not been studied in great detail from the physical point of view. Standard nonlinear theories of spinodal decomposition such as that of Langer, Bar-on, and Miller [20] do not seem applicable in $d = 1$: since they are based on the competition between locally ordered equivalent stable states they do not include the competition between different wave numbers [21], which seems essential in $d = 1$. For the Cahn-Hilliard equation in $d = 1$ we have also an initially periodic structure which coarsens in time to approach $q = 0$. The main difference with our model is that the spatial integral of $\theta(x)$ is conserved by the Cahn-Hilliard equation, so that a completely uniform solution cannot be approached unless $\int dx\,\theta(x, t = 0) = 0$. In the generic case, the final state is the coexistence of two domains of the stable phases and not only one as in our case. Thus, the final stages of evolution should be very different in both models [11]. The fact that, in addition to the fastest growing mode, the mode with $q = 0$ is also linearly unstable in (1) implies a wide range of unstable wave numbers in the initial regime, leading to a wide spectrum during the nonlinear stages. Time-dependent configurations do not approach closely any of the unstable periodic solutions. The consequence is that theories such as that of Langer [22] assuming that the system is close to one of the stationary unstable solutions at each time, will be only of certain usefulness at extremely long times [11], where the mode with $q = 0$ will be the dominant one.

III. NUMERICAL STUDY OF TRANSIENT DYNAMICS FOR LARGE SYSTEMS

The time evolution of $\theta(x,t)$ from an initial condition close to the unstable steady state $\theta(x) = 0$ has been calculated by solving numerically Eq. (1) on a grid of N points with periodic boundary conditions. In the remaining part of the paper, we fix the value of the parameters in (1) to $a = 0.002$, $b = 3$, and $c = 1$ as appropriate for typical values of the parameters in the nematic hydrodynamic equations [8, 13]. In this case $q_m = 0.7$. We have used a centered finite-difference scheme up to order $(dx)^4$ to approximate the spatial derivatives. A predictor-corrector method with one step has been used to determine θ at $t + dt$. A suitable value for dx has been determined integrating the equation in the linear regime and comparing the growth rate of the unstable modes obtained numerically with the one calculated analytically. A value of $dx = 0.25$ has been thereby chosen. The most unstable mode has a wavelength of $\lambda_m = 2\pi/q_m \approx 8.98$,

which corresponds to approximately 36 grid points. The length of the system is $L = Ndx$. We have considered a range of system sizes from $L = 64$ to $L = 256$ and we have always taken periodic boundary conditions. The time step used is 10^{-4}. For dt larger than 0.004 numerical instabilities were observed. For values of dt ranging from 2×10^{-4} to 5×10^{-5} the discrepancies in $\theta(x)$ after five units of time of integration were smaller than 10^{-7}.

The initial condition is written as

$$\theta(x,0) = \sum_{q_n} \theta_{q_n}(0) e^{iq_n x} , \tag{17}$$

where the sum is over modes $q_n = 2\pi n/L$ and it has been taken to run only over the unstable modes $-q_c < q_n < q_c$. As we are interested in the mode competition, all the unstable modes were given the same initial amplitude ϵ. Since $\theta(x)$ has to be real we took $\theta_{q_n}(0) = \theta^*_{-q_n}(0) = \epsilon e^{i\phi_{q_n}}$, where ϕ_{q_n} is a random phase shift for $n \neq 0$ and ϕ_{q_0} is 0 or π. To obtain different initial configurations of $\theta(x)$ the set of random-phase shifts ϕ_{q_n} was changed but not the amplitude ϵ, which remained fixed to the value $\epsilon = 10^{-4}$. Hence, when talking about a different initial condition we mean a different set of random-phase shifts. This choice gives a null ensemble average of $\theta(x)$. All the averages considered in this paper are understood as ensemble averages over different initial configurations.

In addition to our transient dynamics study, we have also examined the existence of periodic stationary solutions [type (c) in Sec. II]. Starting with a configuration of the form $\theta(x) = \epsilon \sin(q_n x)$ involving a single mode $q_n < q_c$ with an amplitude $\epsilon = 2 \times 10^{-4}$, the pattern develops with the growth of its harmonics until a stationary pattern is obtained. We know that this pattern is unstable and the velocity of its decay has been tested numerically by adding a small amplitude to all the modes with q smaller than q_c. The decay was found to be always extraordinarily slow. This means that these unstable stationary solutions can be long lived. When the initial condition (17) is used, the pattern develops in a way that none of these periodic stationary patterns is approached during the transient dynamics provided the system size is large enough (see next section).

Our results for the transient dynamics study are summarized in Figs. 2, 3, and 4 for the evolution of the configuration $\theta(x,t)$, the associated structure factor, and the number of rolls of the pattern respectively. General features of the time evolution that manifest themselves in specific ways in these figures are the following: A linear and a nonlinear regime of evolution can be clearly identified. In the linear regime the pattern is formed. In the nonlinear regime no mechanism of wavelength selection occurs, but domains of a characteristic size exist. These domains include several rolls and evolve in time in a way essentially independent of each other.

In Fig. 2(a), the time evolution of the pattern $\theta(x)$ for a particular initial condition is shown. The periodicity related to the linearly most unstable mode becomes apparent on $\theta(x)$ in the initial stages. Afterwards, we observe that rolls disappear continuously. The presence of regions of different periodicities can be observed. For

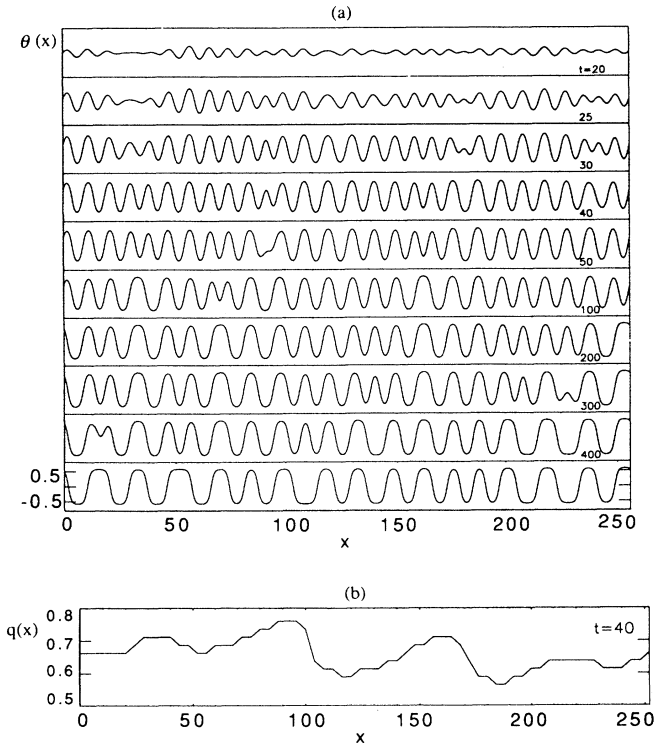

FIG. 2. (a) Time evolution of $\theta(x)$ from a particular initial condition and $L = 256$. The vertical scale is the same for all times. (b) Local wave number $q(x)$ for the configuration at $t = 40$ of (a).

example, at $t = 40$ around seven of these regions are distinguished. A systematic method of identifying such regions is to find the power spectra of small regions in the pattern, and identify the maxima in these local spectra with a dominant local wave number [2]. Explicitly, we have multiplied the configurations in Fig. 2(a) times a Gaussian of width $\sigma = 10$, unit height, and centered at x. Then we have calculated the maxima in the power spectra of such localized patches as a function of x. Figure 2(b) shows the result of one of such analysis, at time $t = 40$, identifying an x-dependent dominant wave number. At this time the average wave number has already deviated from the linearly most unstable one ($q_m = 0.70$) so that one has entered the nonlinear regime. In Fig. 2(a) we can also see that, at each time, a roll is disappearing in that region whose local dominant wave number is largest. Note that the disappearance of a roll occurs locally since this does not affect other regions [compare for example $\theta(x)$ at $t = 100$, 200, and 300]. At the longest times arrived, there are regions were θ is already close to the value of the uniform solution $\theta = \pm b^{-1/2} \approx 0.58$. After this time, it is expected that the pattern evolves towards configurations where regions of $\theta = b^{-1/2}$ and $\theta = -b^{-1/2}$ coexist separated by walls. The separation between these walls will be rather large and the pattern evolution should be described by the theory in [11].

We define the structure factor $S(q,t)$ associated with $\theta(x,t)$ from the discretized configuration $\{\theta(x_n =$

$ndx, t), n = 1, ..., N\}$ as

$$S(q,t) \equiv |\theta_q| . \tag{18}$$

The vertical bars denote the modulus of a complex number and

$$\theta_q \equiv \frac{1}{N} \sum_n e^{-ix_n q} \theta(x_n, t). \tag{19}$$

With this definition, $S(q)$ is independent of system size for a uniform configuration $\theta(x_n, t)$. It is also independent of N during the linear regime. The allowed values of q are of the form $n\,dq$ with n an integer between $-N/2$ and $N/2$ and $dq = 2\pi/L$. Figure 3(a) shows the time evolution of $S(q)$ averaged over 50 independent initial conditions of the form (17). Figure 3(b) shows the time evolution of the area $A(t) \equiv \int dq\, S(q,t)$ for 4 of these independent initial conditions. Since linear theory predicts that the structure factor is independent of the initial phases ϕ_{q_n}, the time at which the different curves in Fig. 3(b) begin to separate signals the end of the linear regime. This happens around $t \sim 20$. During the linear regime the structure factor in Fig. 3(a) is shown to grow with a maximum around the linearly most unstable mode $q_m = 0.7$.

After the linear regime, and reflecting a continuous elimination of rolls, the maximum of $S(q,t)$ shifts towards small q's as times goes on [see Fig. 3(a)]. This continuous drift characterizes the elimination of rolls and it eliminates the idea of a nonlinearly selected wavelength. During the nonlinear regime the structure factor develops important contributions for short and long

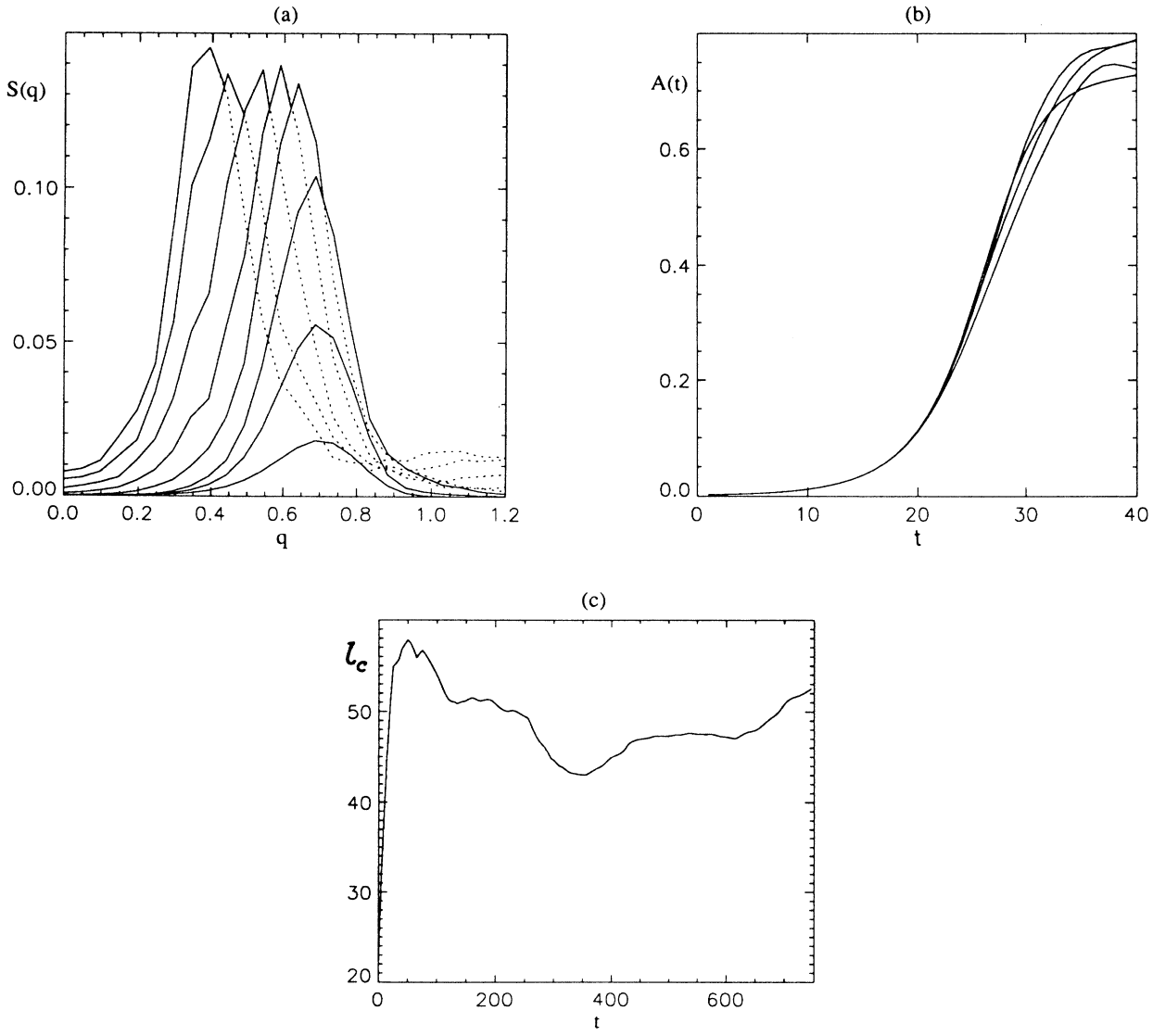

FIG. 3. (a) Time evolution of the structure factor averaged over 50 runs for $L = 128$. Times showed are, from bottom to top, $t = 20$, 25, 30, 50, 100, 200, 500, and 750. (b) Area $A(t)$ of $S(q,t)$ for four independent runs ($L = 128$). (c) Correlation length l_c as a function of time (see text for details).

wavelengths which indicate the existence of strong competition between many modes. The existence of different domains in the configuration $\theta(x,t)$ can be characterized from the structure factor by defining a correlation length $l_c = 2\pi/w$, where w is one half of the width of the peak of the averaged $S(q,t)$ at its mean height. This length has been plotted in Fig. 3(c) for a system of size $L = 128$. It is around 1/3 of the system length for this system size. Hence, we talk about approximately three uncorrelated zones in the system which evolve independently. The validity of this view is enhanced by the evolution observed in systems with $L = 256$, as discussed above, and also with $L = 64$: w turns out to be roughly independent of system size and time (during the nonlinear regime we consider here). The domain size is probably determined by the interplay between the intensity ϵ of the initial condition and the shape of $\omega(q)$.

Figure 4 shows the average number of zeros per unit length of $\theta(x)$ as a function of time. This quantity identifies the number of rolls per unit length of the pattern and it measures the "average" wave number in the system. The inset in this figure represents the average over initial conditions of the number of zeros per unit length versus a mean wave number defined as $\langle q \rangle \equiv \int qS(q,t)dq/A(t)$. The upper part of the curve in the inset corresponds to the very early initial regime. Beyond this regime the number of zeros is linearly related to $\langle q \rangle$, so that a description in terms of any of these quantities is equivalent. The number of zeros per unit length is seen to grow during the linear regime of pattern emergence reaching a value around 0.22, which corresponds to the global wave number selected by fastest linear growth, $q_m = 0.7$. This number of zeros remains constant for a little while beyond the end of the linear regime at $t \sim 20$. Later the average number of zeros decreases monotonically in time making again clear that we cannot identify any nonlinearly selected wave number. This result is different from the one found in Ref. [8] for a similar system. We will

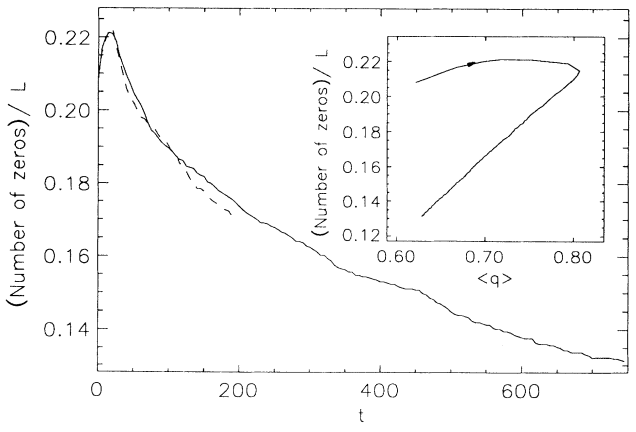

FIG. 4. Number of zeros per unit length in $\theta(x)$ vs time for $L = 128$ (solid line) and $L = 256$ (dashed line). In the inset the same quantity is plotted vs $\langle q \rangle$ (for $L = 128$). For $L = 128$ and 256 an average over 50 and 20 initial conditions, respectively, was taken.

show in Sec. IV that an apparent wavelength selection might occur due to finite-size effects. We have attempted to obtain a growth law for the decay process in Fig. 4. The decay is certainly slower than the one given by a power law. A relation $\langle q \rangle = 21.3 - 1.27 \ln t$ seems to fit the curve for $t \geq 90$. Nevertheless, a decay $(\ln t)^{\beta}$ could also be fitted. Determining the exact law and an accurate exponent will need a considerable increase in the statistics and it is not our goal here. We note that a logarithmic decay is the one expected from one-dimensional domain-wall dynamics [11, 22], but the largest times in our simulations are still far from the regime in which the pattern is composed of domains of the equilibrium phases separated by thin walls.

An important question in relation to the existence of domains of a characteristic size is the dependence of the transient dynamics on the system size L. It is already seen in Fig. 4 that the evolution of the number of zeros per unit length is essentially the same for two system sizes. We have checked that the time scales of evolution are independent of system size for $L \gtrsim 50$. Taking advantage of this fact, a systematic study of the dependence on L of the temporal evolution of the structure factor can be carried out by the analysis of the evolution of the area A of the averaged $S(q,t)$. This area is shown in Fig. 5(a) for systems of different size. From $t = 75$ to the longest time considered ($t = 200$), a relationship of the form $A(L,t) = L^{\alpha} f(t)$ is satisfied, with $\alpha = -0.49 \pm 0.01 \approx 1/2$, for system sizes large enough. Figure 5(b) shows the validity of this size-dependent behavior. The combination of this result with the existence of size-independent time scales of evolution implies that the dependence of the structure factor on system size factors out:

$$S(q,t,L) = L^{-1/2} F(q,t) \; . \tag{20}$$

This finite-size scaling form contrasts with the one found in the dynamics of order-disorder transitions and of spinodal decomposition [23] in $d \geq 2$, where the scaling function F depends on system size as $F(qL, t/L^z)$, and the exponent α is 0 instead of $-1/2$. The reason for such difference can be elucidated by noting that the exponent $\alpha = -1/2$ is a manifestation of the fact that the system is composed of uncorrelated regions of a size independent of the system size. This can be seen from the following argument: If the system is made of many uncorrelated regions, the law of large numbers implies that the sum in (19) approaches a Gaussian variable of standard deviation proportional to the square root of the number of independent zones. Since the size of the zones is independent of L, this standard deviation is proportional to $L^{1/2}$. The average of the modulus of a complex Gaussian variable is proportional to its standard deviation, and the normalization factor $1/N = dx/L$ present in definition (19) completes the factor $L^{-1/2}$ in (20). This argument confirms again the important dynamical role of the "domains of different wave number" identified before. To further stablish this picture, we note that the law $A \sim L^{-1/2}$ should fail when there is only one or less than one domain in our system. According to the results

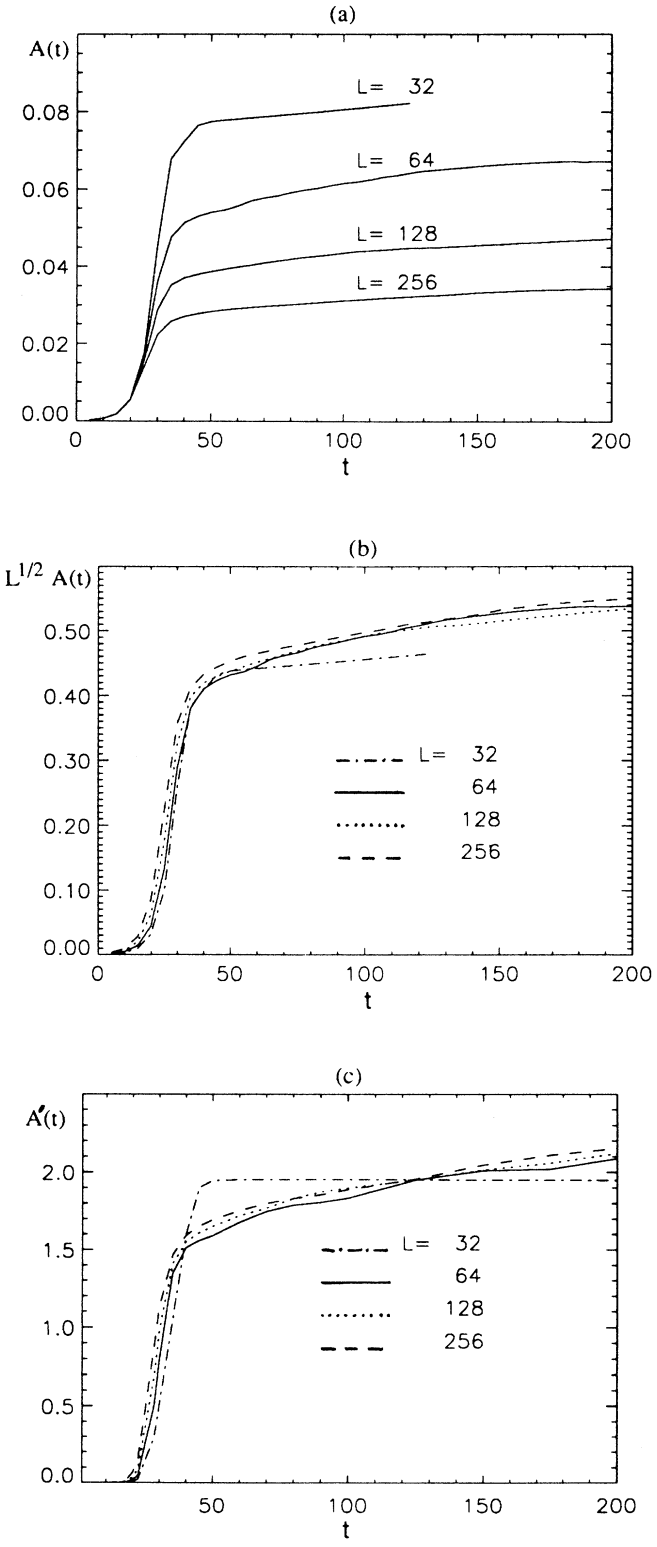

FIG. 5. (a) Area of the averaged $S(q)$ as a function of time for systems of different sizes. For size $L = 128$ the structure factor has been averaged over 50 different initial conditions. For the other system sizes the average is over 20 initial conditions. (b) The same area scaled by $L^{1/2}$. (c) Area of the average over 40 initial conditions of $S'(q,t)$ in Eq. (21).

of Fig. 3(c), this will happen for $L \leq 50$ ($N \leq 200$). This has been checked with a system of size $L = 32$ ($N = 128$) so that it is well described by a single local wave number during the time interval included in Fig. 5(b).

It should be stressed that although the precise value found for α, $\alpha = -1/2$, is a consequence of the definition (18) and (19) used for the structure factor, the factorization of the L dependence of the structure factor is not a trivial consequence of such definition, but rather it reflects the physics of uncorrelated regions described above. Indeed, if one uses an alternative definition of the structure factor:

$$S'(q,t) \equiv N\,|\theta_q|^2 \ , \tag{21}$$

the argument above implies that for large enough systems and after the linear regime, a factorization such as (20) should hold, but with $\alpha = 0$. Such a relation contrasts again with the result for the description of order-disorder transitions and spinodal decomposition in $d \geq 2$ for which $S'(q,t) = L^d F(qL, tL^z)$ [23]. To provide further evidence of the factorization of the L dependence of the structure factor we show in Fig. 5(c) the average of the area $A'(t)$ of $S'(q)$ over 40 different initial conditions for systems of different size. As predicted, no size dependence ($\alpha = 0$) is found after the linear regime for systems of $L = 64$, 128, or 256. However, $A'(t)$ for a smaller system ($L = 32$) deviates from the behavior found for larger systems indicating the breakdown of a relation such as (20) (now with $\alpha = 0$) for small systems. A discussion of the dynamics of these small-size systems is given in Sec. IV.

In the dynamics of conventional phase transitions such as order-disorder transitions or spinodal decomposition in $d \geq 2$ one can also identify independent domains containing some "ordered phase." The difference with our model is that in the usual case such an ordered phase is close to an equilibrium stable phase. Then domains growth and coalesce until one (or two in the case of spinodal decomposition) of them reaches the size of the whole system. This domain growth and saturation produces the t/L^z dependence of the scaling function in time. In our case, the domains contain an "unstable periodic phase," so that there is no driving force for growth, and the domains keep their size roughly constant [see Fig. 3(c)], but continuously reduce their wave number by local roll destruction. This process will presumably continue until each domain contains only one of the uniform stable phases $\pm b^{-1/2}$ and then a growth of the domains similar to that in the model (16), as described in [11], is expected.

IV. SMALL SYSTEMS

Following our discussion above, we will call a system "small" when its size is smaller than the correlation length discussed in the preceding section ($l_c \sim 50$), so that it contains effectively only one domain of quite uniform wave number. In this context it is worth reminding here how different characteristics of a system reflect in their Fourier description. First, for a small sys-

tem, modes are more separated than in a larger system ($dq = 2\pi/L$). Second, the difference between a discrete or a continuous (in x) system is that in the first case there is a minimum length dx so that there appears a maximum wave number $2\pi/dx$ and only a finite number of modes is at play if L is finite. In the continuum case ($dx \to 0$), the wave number cutoff goes to infinity and we have an infinity of modes, but their separation continues to be determined by L. As usually recognized, a physically continuous system admits a discrete description of minimum length dx when $2\pi/dx$ is larger than any wave number relevant to the evolution of the system under study.

To study the behavior of "small systems," we have performed numerical integrations of Eq. (1) for a range of values of L for which only three modes are linearly unstable at $t = 0$: $q_n = ndq$, $n = 0, 1, 2$. The mode q_2 is the most unstable one. The explicit results for the amplitude of the three unstable modes and the first linearly stable mode for the case $L = 18$ ($N = 72, dq \approx 0.349$) are shown in Fig. 6(a), as obtained from the direct numerical integration of (1) with the initial condition (17).

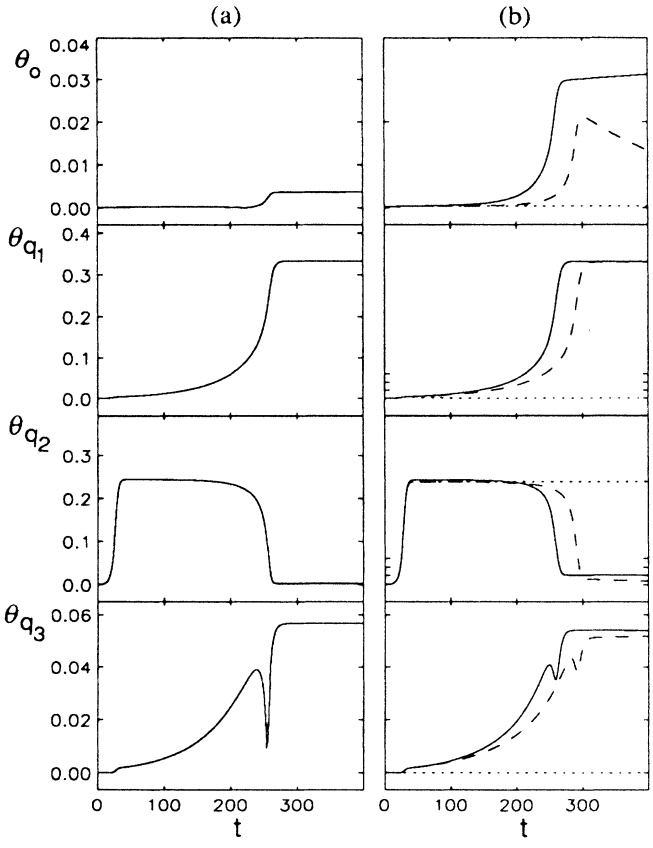

FIG. 6. (a) Amplitudes θ_{q_n} for $n = 0, 1, 2$, and 3 (θ_{q_3} being the first linearly stable mode) obtained by integrating Eq. (1) for a particular initial condition of the form (17) with $L = 18$. (b) The same amplitudes obtained from Eq. (22) (dotted line), from Eq. (22) enlarged to include mode q_3 (dashed line), and including up to mode q_6 (solid line).

The results indicate that the mode q_1 will dominate the pattern for a long time after an initial short regime in which the fastest growing mode q_2 dominates. In such small systems, a well-defined periodicity is observed during a long-time interval, so that an apparent nonlinear selection of the mode q_1 occurs. This happens because the stationary unstable solution $\psi_{q=q_1}$, dominated by a mode and its harmonics, is closely approached during the evolution, in contrast with what we obtain for larger systems. Such configuration is, nevertheless, unstable. The pattern finally decays and the configuration becomes space homogeneous, as expected. This happens at a time $t \sim 1.6 \times 10^5$. This time is not shown in Fig. 6 and should be compared with the time scale in that figure. For such small systems with only three linearly unstable modes, and given that the linearly stable modes have a very small amplitude during the whole time evolution, it is natural trying to describe the dynamics in terms of three coupled ordinary equations for the complex amplitudes θ_0, θ_{q_1}, and θ_{q_2}, all the other amplitudes assumed to be zero. Truncation to a small number of modes is a largely used technique in the literature [24]. Equation (1) is written in Fourier space including only the modes $q_n = ndq$, with $n = 0, 1$, and 2 as

$$\dot{\theta}_{q_n} = \omega(q_n)\theta_{q_n} - b(a + q_n^2) \sum_{i,j=0,1,2} \theta_{q_i}\theta_{q_j}\theta_{q_n - q_i - q_j}. \tag{22}$$

The dependence on system size appears through the values of q_n, which depend on dq.

Equation (22) presents stationary solutions whose stability properties are different from the corresponding solutions of (1). For example, $\theta_{q_2} = [(1 - q_2^2)/(3b)]^{1/2}$ and all the other amplitudes equal to zero are a stationary solution of (22). When the linear stability analysis around this solution is carried out, the result depends on the value of dq: The solution is stable against homogeneous perturbations if $dq < 8^{-1/2} = 0.354$, for any value of a. It is stable against perturbations of wave number q_1 only if $dq < 7^{-1/2} = 0.378$ (this value again is independent of a). This behavior contrasts with the exact properties of Eq. (1), well reproduced by its numerical integration discussed above, for which there are no stable solutions other than the one associated with q_0, *independently* of the value of $dq = 2\pi/L$. The differences in stability properties come from the truncation to a small number of modes, equivalent to replacing the spatially continuous system by a discretized version. Such differences anticipate that a description in terms of a few modes might be qualitatively incorrect. To substantiate this point, we have numerically solved Eq. (22) with $dq = 0.349$, the value associated to $L = 18$, and for which the stability properties of the solutions of (1) and those of the truncated model (22) are different. The same initial value as in the numerical integration shown in Fig. 6(a) was given to the modes included in (22). Figure 6(b) (dotted line) shows that the fastest growing mode q_2 dominates the final state, in contrast with the numerical integration of Eq. (1).

When Eq. (22) is enlarged to include the mode $q_3 =$

$3dq$, which is linearly stable at $t = 0$, the stationary solutions in which only one modal amplitude is different from zero are the same as above, but their stability properties change. For example, the stationary solution dominated by q_2 becomes now unstable for $dq > (10/115)^{1/2} \approx 0.295$ [25]. Numerical solution of (22) including this fourth mode and keeping $dq = 0.349$ shows [dashed line in Fig. 6(b)] that θ_{q_2} decays at $t \sim 300$. Then, a state dominated by q_1 is approached, as in the integration of Eq. (1) but, in contrast with that continuous model, this is here the final asymptotic state. In this state q_3 is slightly developed and the other modes have a small amplitude. Again, this is a stable solution of the set of four equations and the mode $q = 0$ is not yet reached. Figure 6 (solid line) shows that inclusion of up to seven modes alters the time scales, but not the qualitative picture.

As a conclusion, using only the set of linearly unstable modes, or only some additional ones, is not enough to describe the time evolution of the continuous system (which we expect to be well described by the simulations with 72 grid points, equivalent to 72 modes). A large number of linearly stable modes are relevant, although their amplitudes always remain very small. It is worth noting that sets of equations containing the linearly unstable modes or only a few more are often used with success in the literature [1, 24]. The source of success in these cases is not usually explicitly stated. It becomes clear from the discussion of the example above that the truncation to the set of linearly unstable modes can be useful, at most, when these modes are associated with stable stationary solutions of the problem. Otherwise, such truncations can produce incorrect results.

ACKNOWLEDGMENTS

We are indebted to Dr. J. Viñals for many useful suggestions, invaluable discussions, and for his help in solving problems associated with the numerical procedures. Useful discussions with Dr. P. Coullet and Dr. D. Walgraef are also acknowledged. This work has been partially supported by Dirección General de Investigación Científica y Técnica (DGICyT, Spain), under Contract No. PB 89-0424 and a grant from NATO, within the program "Chaos, Order and Patterns: Aspects of Nonlinearity," Project No. 890482.

[1] Contributions by A.C. Newell and G. Ahlers, in *Lectures in the Sciences of Complexity*, edited by D.L. Stein (Addison-Wesley, Redwood City, CA, 1989); *Propagation in Systems Far from Equilibrium*, edited by J.E. Wesfried, H.R. Brand, P. Manneville, G. Albinet, and N. Boccara (Springer-Verlag, Berlin, 1988); contributions by P.C. Hohenberg and M.C. Cross, in *Fluctuations and Stochastic Phenomena in Condensed Matter*, edited by L. Garrido (Springer-Verlag, Berlin, 1987).

[2] J. Viñals, E. Hernández-García, M. San Miguel, and R. Toral, Phys. Rev. A **44**, 1123 (1991); J. Viñals, H.-W., Xi and J.D. Gunton, Phys. Rev. A **46**, 918 (1992); K.R. Elder, J. Viñals, and M. Grant, Phys. Rev. Lett. **68**, 3024 (1992).

[3] M. San Miguel and F. Sagués, in *Patterns, Defects and Materials Instabilities*, edited by D. Walgraef and N.M. Ghoniem (Kluwer, Dordrecht, 1990).

[4] B.L. Winkler, H. Richter, I. Rehberg, W. Zimmermann, L. Kramer, and A. Buka. Phys. Rev. A **43**, 1940 (1991).

[5] E. Guyon, R. Meyer, and J. Salan, Mol. Cryst. Liq. Cryst. **54**, 261 (1979).

[6] M. San Miguel and F. Sagués, Phys. Rev. A **36**, 1883 (1987).

[7] A. Buka and L. Kramer, Phys. Rev. A **45**, 5624 (1992).

[8] G. Srajer, S. Fraden, and R.B. Meyer, Phys. Rev. A **39**, 4828 (1989)

[9] P.G. de Gennes, *The Physics of Liquid Crystals* (Clarendon, Oxford, 1975).

[10] J. Swift and P.C. Hohenberg, Phys. Rev. A **15**, 319 (1987). This equation was originally introduced to describe Rayleigh-Bénard convection near threshold.

[11] F. Sagués and M. San Miguel, Phys. Rev. A **39**, 6567 (1989)

[12] M.O. Cáceres, F. Sagués, and M. San Miguel, Phys. Rev. A **41**, 6852 (1990).

[13] Equation (1) can be related to the simplified nematodynamic equations in the form $\dot{\theta} = (a_1 - a_2\partial_x^2)(b_1\partial_x^2\theta + b_2\theta - b_3\theta^3)$, with $a_1 = \gamma_1^{-1}$, $a_2 = d^2(4\pi^2\nu_2)^{-1}(1+\lambda)^2$, $b_1 = K_3$, $b_2 = \chi_a H^2 - K_2(\pi/d)^2$, and $b_3 = \chi_a H^2/2$. The meaning and the typical values of the parameters involved can be found in [8]. If a rescaling is performed $\theta' = b_2\theta$, $x' = (b_2/b_3)^{1/2}x$, and $t' = b_2^2 a_2/b_1 t$, Eq. (1) with $c = 1$ is eventually obtained with $a = 0.02$ and $b = 3.0$ for an assumed magnetic field of $H = 8$ kG.

[14] J.D. Gunton, M. San Miguel, and P. Sahni, in *Phase Transitions and Critical Phenomena*, edited by C. Domb and J.L. Lebowitz (Academic, London, 1983), Vol. 8.

[15] F. Sagués, F. Arias, and M. San Miguel, Phys. Rev. A **37**, 3601 (1988).

[16] J.S. Langer, Ann. of Phys. (N.Y.) **41**, 108 (1967).

[17] See, for example, D.W. Jordan and P. Smith, *Nonlinear Ordinary Differential Equations* (Clarendon, Oxford, 1987), Chap. 9.

[18] K. Kawasaki, M. C. Yalabik, and J.D. Gunton, Phys. Rev. A **17**, 455 (1978); F. de Pasquale, P. Tartaglia, and P. Tombesi, *ibid.* **31**, 2447 (1985); K. Elder and M. Grant, J. Phys. A **23**, L803 (1990).

[19] P.C. Hohenberg and B.I. Halperin, Rev. Mod. Phys. **49**, 435 (1977).

[20] J.S. Langer, M. Bar-on, and H.D. Miller, Phys. Rev. A **11**, 1417 (1975).

[21] M. Grant, M. San Miguel, J. Viñals, and J.D. Gunton, Phys. Rev. B **31**, 3027 (1985).

[22] J.S. Langer, Ann. Phys. (N.Y.) **65**, 53 (1971). (1977).

[23] J. Viñals and D. Jasnow, Phys. Rev. B **37**, 9582 (1988); H. Guo, Q. Zheng, and J.D. Gunton, *ibid.* **38**, 11547 (1988).

[24] See, for example, L. Kramer, H.R. Schober, and W. Zimmermann, Physica D **31**, 212 (1988); R.D. Benguria and M.C. Depassier, Phys. Rev. A **45**, 5566 (1992).

[25] Note that a value $dq = 0.295$ is in the range $dq < 1/3$ in which there are more than three unstable modes and a description in terms of only three modes is already *a priori* inadequate.